

Combustion Behavior of Animal-Manure-Based Hydrochar and Pyrochar

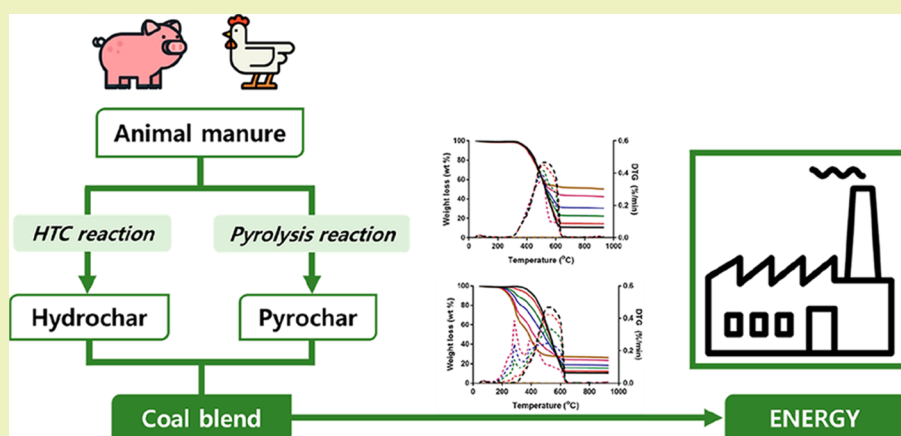
Kyoung S. Ro,^{*,†} Judy A. Libra,[‡] Sunyoung Bae,[§] Nicole D. Berge,^{||} Joseph R.V. Flora,^{||} and Ralf Pecenka[‡]

[†]USDA-ARS Coastal Plains Soil, Water, and Plant Research Center, Florence, South Carolina 29501, United States

[‡]Leibniz Institute for Agricultural Engineering and Bioeconomy, Max-Eyth-Allee 100, 14469 Potsdam, Germany

[§]Chemistry Department, Seoul Women's University, Seoul 01797, Korea

^{||}Civil and Environmental Engineering, University of South Carolina, Columbia, South Carolina 29201, United States



ABSTRACT: The sustainability of energy production can be increased by combusting waste-derived solid fuels, alone or as blends with coal. This paper investigated whether two thermochemical processes (hydrothermal carbonization and pyrolysis) can be used in sustainable manure management systems to convert surplus manure waste streams into renewable fuels. Hydrochars and pyrochars derived from swine manure and poultry litter at various process conditions were characterized. Their combustion behavior was studied by thermogravimetric analysis, individually and simulated as a blend with fossil coal. The hydrochars underwent two combustion stages, active and char combustion, while the pyrochars and four fossil coals showed only one stage. The substantial differences in characteristic combustion temperatures, kinetic parameters, and ash content between animal-manure-derived chars and coal suggest that fossil coals should not be replaced entirely with char, but used preferably as a blend. Simulation of blends with coal showed combustion characteristics similar to coal alone with amounts up to 10% (hydrochar) and 80% (pyrochar). Although more scale-up and ash characterization study is needed before implementation, the results suggest high potential of cocombusting small percentages of animal-manure based hydrochar and pyrochar with coal in existing coal power generation facilities.

KEYWORDS: Livestock waste, Hydrochar, Pyrochar, Fossil coal, Combustion characteristics

INTRODUCTION

Massive consolidation of animal feeding operations has been taking place over the past decades, resulting in more and more concentrated animal feeding operations (CAFOs) in the U.S. and worldwide. With these CAFOs, new, more effective manure management systems are required to make the animal feeding operations economically viable and environmentally benign. The amount of manure produced often exceeds the local demand for nutrient recycle to agricultural land, leading to pollution and nuisance problems. The composition of manure can be highly variable, depending on the type of animal, diet, feed composition, housing system, and manure management (type of bedding material, reuse/removal

frequency, storage, and handling). Besides the organic animal and feed wastes, manure contains plant nutrients (e.g., N, P, K, Ca, Mg, S), trace elements (e.g., Cu, Zn, As), pesticide/pharmaceutical residues, and microorganisms.^{1,2} The potential use of animal manures as bioenergy feedstocks for waste-to-bioenergy conversion has been reported in the literature, via combustion^{3–5} and via thermochemical conversion processes such as wet and dry gasification and pyrolysis.^{6–18} Difficulties in using manure as a fuel comes from its relatively high

Received: August 9, 2018

Revised: November 9, 2018

Published: December 3, 2018

moisture content (e.g., poultry litter: 5–40%, swine solids: 66–97%), low bulk and energy densities, variable chemical composition, and high ash content.^{19,1,14,20} The low bulk density limits how far manures can be economically transported for use as fuel or fertilizer.⁴ In addition, the chemical composition of animal manures can be very different than coal.^{21,22} Increased contents of Cl, N, and S, typical for agricultural biomasses, can lead to problems in boilers or downstream components, such as metal corrosion (Cl), interfere with catalytic processes removing NO_x and SO_x (As) or, in systems with no emission control, can cause higher emissions of NO_x, HCl, and SO_x.²³ Furthermore, the high amount of ash-forming elements can lead to so-called “slagging” and “fouling”, requiring more cleaning operations for the boiler and heat exchangers to avoid disturbances and reductions in efficiency. Therefore, a modification of biomasses before energetic use with the target to produce a fuel with coal-like properties is a needed prerequisite for the use of manures as a fuel in coal-fired plants without modifications of the boiler installations.

Hydrothermal carbonization (HTC) is an emerging thermochemical conversion technique that can be used to modify animal manures to a char with relatively high energy values and ash contents, which can be combusted to generate heat and power. HTC has been shown to produce carbon-rich char called hydrochar from wet feedstock with fewer energy requirements than traditional dry pyrolysis.²⁴ The HTC reactions occur in a closed system at relatively low temperatures (180–250 °C) in the presence of water or steam under autogenic pressures. Berge et al.²⁵ reported that HTC is a low-energy carbon conversion/waste treatment technology well suited to manage wet feedstock streams, as the predrying prior to processing is not required. The high heating value of hydrochar makes HTC competitive to other carbon forms such as lignite.²⁶ The hydrochar made from animal manures showed high carbon and ash contents.²⁷

Although HTC was originally developed to produce coal-like material from biomass, little work investigating the combustion characteristics of animal-manure based chars has been conducted to date.²⁸ Understanding the combustion behavior of these chars is also important when developing cofiring strategies, which may be necessary if utilizing existing combustion infrastructure. Co-combustion of manure-derived chars and coal has also not been investigated with great depth. However, the effects of cofiring woody biomass, with its higher fraction of hydrogen and oxygen and less carbon than coal, in coal-burning facilities has often been studied.^{29–31} The differences in composition are connected not only with a lower heating value but also with a higher content of volatile matter. Whereas bituminous coal has a much higher heating value than woody biomass (27–30 MJ kg⁻¹ vs 18–21 MJ kg⁻¹), the content of volatiles in coal is much lower (32–37 wt % vs 76–86 wt %).

The specific objectives of this study were to determine the combustion characteristics and kinetics of animal-manure based hydrochar and compare them to those of pyrochar from the same feedstocks. Estimates of how the combustion characteristics will be affected by the blending of these chars with coal for power generation were made by simulating the combustion kinetics using the experimental data.

MATERIALS AND METHODS

Animal Manure Feedstock and Fossil Coals. The raw swine solids (RSS) were obtained from a solid–liquid separation system treating flushed manure from a 5600-head finishing swine operation in North Carolina. Raw poultry litter (RPL) was obtained from a 52 000-bird broiler farm with dirt flooring in South Carolina. These manures were dried in a greenhouse, milled to pass through a 1 mm screen, and stored in a refrigerator at 4 °C prior to use. Four fossil coal samples were obtained from a local power plant for comparison purposes.

Hydrochar Production. Tubular reactors (2.54 cm diameter × 25.4 cm long) constructed with 304/304L stainless steel pipe were used to produce hydrochars. Hydrochars from swine solids (HSS) were produced at two feedstock solids contents (20% and 50% total solid or TS), two HTC temperatures (200 and 250 °C), and two reaction time periods (4 and 20 h). Poultry litter hydrochars (HPL) were produced with two feedstock solids contents (20 and 50% TS) at 250 °C for 20 h of reaction time. The hydrochars are referred to throughout with abbreviations that include the feedstock, % solids, HTC temperature, and reaction time (e.g., HSS.20%.200C.4h). More detailed information about the reactor systems and hydrochar production can be found elsewhere.³²

Pyrochar Production. Pyrochar was produced from dried swine solid (PSS) and poultry litter (PPL) pellets. Pelletizing the manures involved drying to 105 °C, grinding the dry manure to 2 mm particle size, rehydrating the manure to moisture contents of 20–30%, then creating 6 mm pellets. These raw feedstock pellets were pyrolyzed using a Lindburg electric box furnace equipped with a gastight retort (Model 51662, Lindburg/MPH, Riverside, MI). This particular furnace-retort had a specially modified setup³³ to ensure precision regulation of the final charring temperature. The temperature schedule used for pyrolysis involved the following: (1) Hold for 60 min and purge using 15 L min⁻¹ industrial-grade N₂ at 200 °C for equilibration; (2) Ramp up to the desired pyrolytic temperature while dropping N₂ flow to 1 L min⁻¹ within 60 min (2.5 °C min⁻¹ for 350 °C runs, 5.0 °C min⁻¹ for 500 °C runs); (3) Hold for 120 min at the desired temperature for equilibration; and (4) Cool at 4.25 °C min⁻¹ to below 50 °C then purge before withdrawing the pelletized biochar samples. The pyrochars are referred to throughout with abbreviations that include the feedstock, pyrolysis temperature, and reaction time (e.g., PSS.350C.2h).

Proximate and Energy Content Analyses. Proximate analyses of solid samples were performed using the thermogravimetric method.³⁴ Higher heating values (HHV) of feedstock, hydrochar, and pyrochar samples were measured using a LECO AC500 Isoperibol Calorimeter (LECO Corp., St. Joseph, MI) following ASTM standard D 5865.³⁵

Thermogravimetric Analysis. Thermogravimetric analysis (TGA-DTA analyzer, TGA/SDATA851e, Mettler Toledo International, Inc., Columbus, OH) with air was used to determine combustion characteristics of hydrochar, pyrochar, and coal samples obtained from a local coal power plant. All samples (weight range from 10 to 15 mg) were placed in an Al₂O₃ 70 μL crucible and combusted under a zero-grade air atmosphere (i.e., 21.5% O₂, 78.5% N₂, total hydrocarbons <1 ppm), with an air flow rate of 60 mL min⁻¹, over a temperature range of 50 to 890 °C, and a constant heating rate of 10 °C min⁻¹.

The weight loss profiles of animal manure solids provide information about both combustion temperatures and kinetics. Three combustion characteristic temperatures were determined:^{36,37} ignition temperature (T_{ig}), burnout temperature (T_b), and peak temperature (T_p). The ignition temperature, the temperature at which fuels started burning, was defined as the temperature at which the combustion rate raised to 1 wt % min⁻¹ at the start of a major combustion process. The temperature at the peak of the derivative thermogravimetric (DTG) curve was defined as the peak temperature. The burnout temperature, the temperature at which combustion reaction stopped, was defined as the temperature at which

Table 1. Experimental Results for the Two Feedstocks at Different Temperatures, Percent Solids, and Reaction Times: Solid and Energy Yields as a Percentage of Initial Feedstock Mass and Energy Content, Proximate and Ultimate Analyses^a

| sample | solid yield (%) | energy content (MJ kg ⁻¹) | energy recovered (%) | proximate analysis | | | | | |
|--------------------------|-----------------|---------------------------------------|----------------------|--------------------------|-----------------|------|--------|------|-------|
| | | | | VM ^b | FC ^c | | ash | | |
| | | | | (wt %, db ^d) | | | | | |
| raw swine solids (RSS) | - | 19.5 (0.2) | - | 69.5 | (1.1) | 9.3 | (0.8) | 21.2 | (0.3) |
| raw poultry litter (RPL) | - | 13.0 (0.3) | - | 56.8 | (0.5) | 9.1 | (0.5) | 34.0 | (0.5) |
| Hydrochars | | | | | | | | | |
| HSS.20%.200C.4h | 65 (3.3) | 20.6 (1.3) | 69 (4.4) | 61.8 | (0.9) | 12.5 | (1.0) | 25.7 | (0.5) |
| HSS.20%.250C.4h | 76 (2.1) | 19.7 (0.3) | 76 (1.0) | 65.3 | (1.9) | 12.0 | (2.0) | 22.8 | (0.7) |
| HSS.20%.200C.20h | 58 (2.4) | 22.3 (0.4) | 67 (3.0) | 56.7 | (1.1) | 14.9 | (1.5) | 28.5 | (1.1) |
| HSS.20%.250C.20h | 60 (2.5) | 21.6 (0.7) | 66 (0.6) | 59.8 | (1.8) | 13.7 | (2.3) | 26.5 | (1.5) |
| HSS.50%.200C.4h | 56 (1.9) | 18.6 (0.6) | 54 (3.1) | 54.0 | (1.7) | 13.5 | (2.0) | 32.5 | (1.0) |
| HSS.50%.250C.4h | 73 (9.7) | 18.7 (0.2) | 70 (9.8) | 61.5 | (0.8) | 13.1 | (1.3) | 25.5 | (1.0) |
| HSS.50%.200C.20h | 53 (3.6) | 19.5 (0.3) | 54 (4.2) | 51.1 | (1.3) | 14.4 | (1.7) | 34.5 | (1.1) |
| HSS.50%.250C.20h | 68 (1.4) | 18.4 (0.2) | 64 (1.8) | 58.9 | (1.6) | 13.8 | (2.3) | 27.3 | (1.6) |
| HPL.20%.250C.20h | 60 (1.9) | 11.6 (0.8) | 53 (2.6) | 39.8 | (11.0) | 17.3 | (14.2) | 42.9 | (8.9) |
| HPL.50%.250C.20h | 68 (0.8) | 10.3 (1.2) | 54 (6.0) | 39.2 | (6.0) | 14.8 | (8.9) | 46.0 | (6.5) |
| Pyrochars | | | | | | | | | |
| PSS.350C.2h | 51.8 | 16.0 (0.1) | 60 | 31.7 | (0.3) | 26.6 | (0.4) | 41.8 | (0.3) |
| PSS.500C.2h | 41.9 | 13.8 (0.1) | 42 | 17.1 | (0.2) | 33.4 | (1.5) | 49.4 | (1.5) |
| PPL.350C.2h | 45.6 | 16.0 (0.2) | 53 | 33.5 | (1.0) | 30.8 | (1.4) | 35.7 | (0.9) |
| PPL.500C.2h | 37.6 | 14.8 (0.5) | 41 | 20.3 | (0.9) | 37.5 | (1.2) | 37.5 | (0.9) |
| Fossil Coal Samples | | | | | | | | | |
| Coal1 | - | 29.2 (0.2) | - | 32.0 | (0.2) | 57.4 | (0.3) | 10.6 | (0.2) |
| Coal2 | - | 28.7 (0.1) | - | 34.8 | (0.0) | 55.7 | (0.1) | 9.5 | (0.0) |
| Coal3 | - | 29.4 (0.1) | - | 32.0 | (0.1) | 55.9 | (0.1) | 12.1 | (0.1) |
| Coal4 | - | 29.5 (0.1) | - | 33.3 | (0.0) | 57.7 | (0.2) | 9.0 | (0.2) |

^aMean of three replicates with standard deviation in parentheses. ^bVolatile matter. ^cFixed carbon. ^dDry basis.

combustion rate declined to 1 wt % min⁻¹ after major combustion reaction took place.

The TGA weight loss profiles of the hydrochars can be fitted with the following combustion reaction rate equation.¹²

$$\frac{d\alpha}{(1-\alpha)^n} = \frac{A}{\beta} \exp(-E/RT) dT \quad \frac{d\alpha}{(1-\alpha)^n} = \frac{A}{\beta} \exp(-E/RT) dT \quad (1)$$

where

- A = pre-exponential factor (min⁻¹)
- E = activation energy (kJ mol⁻¹)
- R = gas constant (8.314 J mol⁻¹ k⁻¹)
- T = temperature (K)
- n = order of reaction
- $\alpha = \frac{m_o - m_T}{m_o - m_f} = \frac{m_o - m_T}{m_o - m_f}$ = fraction of conversion
- m_o = initial dry mass (g)
- m_T = mass at temperature T (g)
- m_f = final residual mass, consisting of mostly fixed carbon and ash (g)
- β = constant heating rate (K min⁻¹)

Combustion kinetic parameters were estimated similar to that reported for pyrolysis kinetic parameter estimations reported in the literature.^{38,12} Assuming a first-order thermal decomposition reaction for combustion ($n = 1$), eq 1 was rearranged as

$$\ln\left(\frac{d\alpha}{dT} (1-\alpha)^{-1}\right) = \ln\left(\frac{A}{\beta}\right) - \frac{E}{RT} \quad (2)$$

The values of $d\alpha/dT$ and α were obtained from the TGA analysis. The left side of eq 2 was plotted against the inverse of the temperature. A linear model was fitted to each combustion stage with an intercept of (A/β) and a slope of $-E/R$.

Simulated TG and DTG Curves of Banded Feedstocks. The theoretical TG curves of feedstocks blended with either hydrochar or

pyrochar with coals can be simulated by assuming these individual feedstocks undergo combustion reactions independently without interaction.³⁹ The theoretical TG curves were calculated as

$$TG_{\text{theoretical}} = \sum_{i=1}^n z_i(TG)_i \quad (3)$$

where

- i = feedstock I
- n = number of different feedstocks
- $(TG)_i$ = TG of feedstock i
- z_i = mass fraction of feedstock i

The theoretical DTG curves and combustion indices were estimated using the theoretical TG curves.

Statistics. Most experiments were conducted triplicates with a few exceptions. The central tendency and precision of the triplicate measurements were expressed with an arithmetic averages and standard deviations using MS Office Excel (Version 1803).

RESULTS AND DISCUSSION

Yields and Characteristics of Feedstocks and Chars.

The feedstock manures contain a higher amount of ash (21.2 to 34.0%, Table 1) than common lignocellulosic feedstocks, such as wood (typically less than 5%). RPL often has high ash content, often ranging from 20 to 33% depending on the animal diet, litter management technique used, and type of flooring in the sheds (e.g., dirt in this study). The HHV of the RPL was much less than the RSS (13.0 vs 19.5 MJ kg⁻¹) and in line with the average values of 14.3 MJ kg⁻¹ reported by Chastain et al.⁴ In the hydrothermal experiments, the high initial % solids (20–50%) resulted in high solid yields (53–76%), and much of the ash remained in the hydrochar. Increasing the carbonization reaction time from 4 to 20 h (for

swine solids) resulted in a decreased hydrochar yield, but did not affect the ash content significantly. Conversely, the ash became more concentrated in the poultry litter hydrochars (ranging from 22.8 to 34.5% in HSS vs 42.9–46% in HPL). The opposite behavior is observed in the pyrochars (41.8–49.4% in PSS vs 35.7–37.5% in PPL). Both types of solids contain much more ash contents than the fossil coal samples obtained from a local power plant (9–12%). This has an effect on the energy content of the chars; only the 20% swine solids hydrochars and the poultry litter pyrochars have energy contents higher than the respective feedstocks. Both HTC and pyrolysis decreased the volatile matter (VM) and increased the fixed carbon (FC) in the chars. Slightly higher FC values were achieved with longer HTC reaction times.

Comparison of these results to other published studies is complicated by changes in manure composition and carbonization processing conditions. Mau and Gross created hydrochar from poultry litter at slightly different carbonization conditions: 25% initial solids concentration, temperatures ranging from 180 to 250 °C, and a reaction time of 1 h. The results described by Mau and Gross²⁸ indicate a different behavior than observed in this study; the concentration of ash in their hydrochar (from 24.4 in RPL to 30.4% in HPL) did not reduce the energy content of the hydrochar. Instead, it increased from 15.1 for the raw poultry litter to 24.4 MJ kg⁻¹ for hydrochar at 250 °C. This comparison highlights that the properties of raw manures from different sources as well as their behavior in the HTC process can vary greatly. Both raw poultry litters had high ash content (24.4 vs 34.0 wt %, db); however, the ash behavior was not the same in the two hydrothermal treatments.

Combustion Behavior of Animal Manure Chars. The combustion behavior of the raw animal manures and the chars made under various HTC and pyrolysis processing conditions was studied with their thermogravimetric (TG) and derivative thermogravimetric (DTG) curves. Similar to other lignocellulosic biomass, the TG and DTG curves of both raw manures and their hydrochar samples consisted of two main stages of weight loss: active combustion and char combustion (Figure 1a,b). These stages were defined by the peaks in the DTG curves. These dual combustion stages were consistent with other biomass with relatively high volatile matter (VM). The first combustion stage corresponds to devolatilization of VM leading to char formation and the second stage to the high-temperature oxidation of the solid residual.^{31,38} Both combustion stages occurred at similar temperature ranges for the raw poultry litter and its hydrochar samples (Figure 1b). However, the second-stage combustion occurred at a higher temperature for the raw swine manure sample than its hydrochar sample (Figures 1a, 2a).

In contrast to the dual peaks of the raw animal manure and its hydrochar samples, only one broad DTG peak was observed for the coal samples (Figure 2b). The one broad DTG peak of the coal samples at higher temperature was attributed to the simultaneous combustion of VM and char as reported by Toptas et al.³¹ The DTG profiles for all four pyrochars made at two temperatures showed broad peaks more similar to the coal samples (Figure 2c). Park and Jang³⁷ found that pyrochars with low VM made at pyrolysis temperatures at or above 400 °C showed similar broad peak DTG profiles. However, the samples of the raw rice husks and wood pellets as well as those pyrolyzed at 300 °C exhibited two peak DTG profiles.

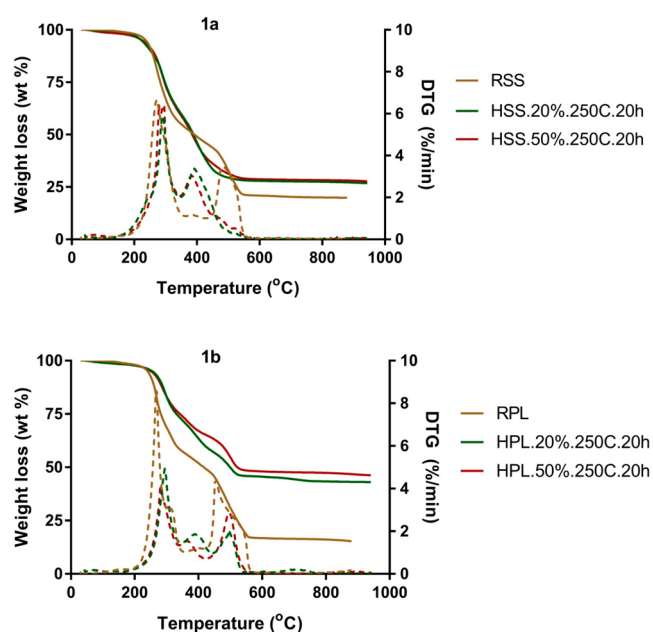


Figure 1. TG-DTG profiles of both raw manure samples and their hydrochars at 250 °C and 20 h: (a) swine manure, (b) poultry litter.

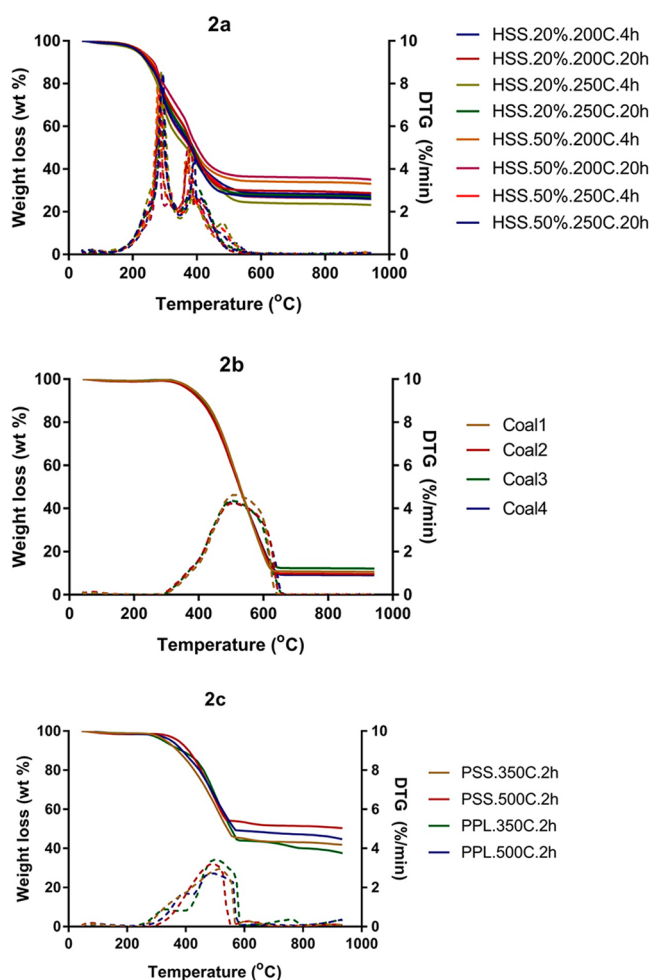


Figure 2. Comparison of the TGA and DTG profiles of (a) all eight swine solids hydrochars at the two temperatures, reaction times and % solids, (b) the four coal samples, and (c) the pyrochars from both animal manures at two temperatures.

Table 2. Combustion Characteristics of Raw Manures, Hydrochars, Pyrochars, and Coals^a

| samples | ignition temperature, T_{ig} (°C) | peak temperature, T_p (°C) | burnout temperature, T_b (°C) |
|------------------|-------------------------------------|------------------------------|---------------------------------|
| RSS | 224 (0.3) | 271 (0.1) | 430 (2.6) |
| RPL | 229 (0.2) | 267 (0.2) | 553 (1.0) |
| HSS.20%.200C.4h | 210 (0.3) | 291 (3.8) | 460 (4.0) |
| HSS.20%.250C.4h | 211 (2.3) | 294 (5.4) | 499 (5.5) |
| HSS.20%.200C.20h | 214 (1.3) | 280 (4.3) | 460 (1.6) |
| HSS.20%.250C.20h | 212 (2.3) | 290 (5.4) | 462 (3.8) |
| HSS.50%.200C.4h | 221(3.8) | 277 (7.5) | 443 (2.1) |
| HSS.50%.250C.4h | 218 (0.4) | 286 (6.9) | 483 (27.3) |
| HSS.50%.200C.20h | 224 (3.2) | 276 (3.9) | 450 (5.0) |
| HSS.50%.250C.20h | 225 (6.3) | 287 (6.6) | 475 (18.9) |
| HPL.20%.250C.20h | 254 (7.2) | 294 (1.4) | 462 (37.9) |
| HPL.50%.250C.20h | 249 (3.2) | 288 (4.3) | 464 (60.4) |
| PSS.350C.2h | 325 (0.9) | 499 (3.6) | 548 (10.2) |
| PSS.500C.2h | 374 (7.6) | 472 (14.5) | 582 (66.5) |
| PPL.350C.2h | 413 (0.4) | 464 (9.5) | 572 (1.3) |
| PPL.500C.2h | 351 (6.4) | 476 (3.0) | 574 (21.2) |
| Coal1 | 372 (1.1) | 514 (2.7) | 623 (3.8) |
| Coal2 | 363 (0.8) | 506 (4.6) | 634 (9.1) |
| Coal3 | 364 (1.4) | 506 (7.5) | 628 (18.2) |
| Coal4 | 362 (1.5) | 499 (2.0) | 639 (15.0) |

^aMean of three replicates with standard deviation in parentheses.

The three characteristic combustion temperatures were determined from the DTG profiles for the char and coal samples as they can have an impact in relation to the required furnace residence time and temperature (Table 2). Ignition temperature is defined as the temperature at which there is a sudden decrease in weight loss, while peak temperature is the temperature that corresponds to the maximum rate of weight loss due to volatilization. Burnout temperature is the temperature on thermograms that shows no further mass loss at the end of the combustion process where fuel weight stabilizes. Comparison of the ignition temperatures shows that the values for the raw manure and its hydrochar samples (210–254 °C) were much lower than those for the fossil coal samples (362–372 °C). Both peak and the burnout temperatures of the raw manure and its hydrochar samples were also lower than those for the coal samples. The lower peak temperatures indicate that the manure and hydrochars are easier to ignite than coal, while the lower burnout temperatures suggest that complete conversion of the manures and hydrochars can be achieved at shorter furnace residence times and lower temperatures. In contrast, pyrolysis increased the three combustion temperatures to ranges similar to fossil coal. These differences in characteristic combustion temperatures were attributed to the large VM fractions in raw and hydrothermally carbonized animal manures. The higher DTG peaks in the first stage also suggested the higher oxidation rate of VM than that for char oxidation in the second stage. Lower ignition temperatures may pose difficulties for the use of hydrochars in existing coal power facilities, as typical coal mills use hot air (e.g., 316 to 343 °C) to dry and transport coal powder to the burner, which could cause a coal mill fire.

Comparison of the results (Table 2) for poultry litter to those of Mau and Gross for hydro- and pyrochar also made from poultry litter shows similar trends for the ignition and peak temperatures; both HTC and pyrolysis increased the two temperatures. While the three combustion temperatures for the raw poultry litter in Mau and Gross were similar to those in this study, carbonization via HTC increased the ignition, peak,

and burnout temperatures for their hydrochar much more than for the sample produced in this study. For example, their ignition temperature increased from 259 to 333 °C vs 229 to 254 °C in this study. These changes highlight the importance of manure composition and carbonization processing conditions on combustion characteristics. Pyrolysis, on the other hand, produced similar combustion temperatures in the two studies.

As discussed above in the section on yields, the properties of raw manures from different sources can vary greatly, which combined with different carbonization process conditions, can cause variations in char properties. Mäkela and Yoshikawa⁴⁰ found that the ash composition, not just ash content, plays an important role in combustion properties. Investigating hydrochar from paper sludge, they found that the reduction in ash content in hydrothermal treatment was caused by dissolution of calcium carbonate. This decreased the ash fusion temperatures, more likely causing incineration problems.

Table 3 shows the kinetic parameters calculated for the two combustion stages for all raw animal manure, the hydrochar samples along with that for a single-stage combustion for the pyrochars and fossil coal samples. The activation energies for the first-stage and the second-stage combustion were different from each other. The activation energy for the swine hydrochars ranged from 67.5 to 77.8 kJ mol⁻¹ for the first stage and 70.0 to 117 kJ mol⁻¹ for the second stage. The activation energies for the poultry litter hydrochar samples were generally higher than that for swine hydrochar samples. The higher second-stage activation energies suggested higher energy was needed to initialize the second-stage combustion. The activation energies for the pyrochar sample ranged from 60.1 to 107 kJ mol⁻¹, while the range for the coal samples was much narrower, 81.9 to 90.1 kJ mol⁻¹. Although HTC was originally developed to produce coal-like material from biomass, the substantial differences in characteristic combustion temperatures and the kinetic parameters between hydrochar and actual coal samples suggests that the fossil coals used by existing coal power plants should not be replaced

Table 3. Summary of Kinetic Parameters: Activation Energy E and Pre-Exponential Factor A ^a

| sample | temp range (°C) | E (kJ mol ⁻¹) | A (min ⁻¹) | R^2 |
|------------------|-----------------|-----------------------------|--|-------|
| RSS | 186–365 | 92.2 (0.1) | 8.8×10^7 (0.1%) ^b | 0.95 |
| | 440–563 | 225 (1.8) | 4.3×10^{14} (28%) | 0.95 |
| RPL | 204–355 | 109 (0.2) | 4.1×10^9 (4.4%) | 0.93 |
| | 434–571 | 182 (5.6) | 5.7×10^{11} (72%) | 0.91 |
| HSS.20%.200C.4h | 151–353 | 70.0 (0.4) | 7.5×10^5 (9.0%) | 0.96 |
| | 354–509 | 117 (2.0) | 1.6×10^8 (29%) | 0.88 |
| HSS.20%.250C.4h | 168–351 | 77.8 (1.5) | 4.7×10^6 (33%) | 0.96 |
| | 355–557 | 86 (2.6) | 3.9×10^5 (42%) | 0.87 |
| HSS.20%.200C.20h | 157–348 | 71.2 (0.6) | 1.1×10^6 (13%) | 0.96 |
| | 349–523 | 99.1 (4.7) | 8.6×10^6 (70%) | 0.84 |
| HSS.20%.250C.20h | 142–351 | 67.5 (1.1) | 4.6×10^5 (25%) | 0.97 |
| | 354–561 | 85.0 (2.5) | 4.2×10^5 (45%) | 0.84 |
| HSS.50%.200C.4h | 142–347 | 67.7 (1.5) | 5.0×10^5 (39%) | 0.97 |
| | 347–558 | 73.8 (1.8) | 6.9×10^4 (32%) | 0.79 |
| HSS.50%.250C.4h | 167–353 | 76.3 (1.0) | 3.0×10^6 (20%) | 0.97 |
| | 354–558 | 81.7 (6.2) | 2.4×10^5 (71%) | 0.84 |
| HSS.50%.200C.20h | 138–305 | 69.5 (1.7) | 1.5×10^6 (40%) | 0.95 |
| | 347–553 | 78.5 (3.8) | 1.9×10^5 (71%) | 0.81 |
| HSS.50%.250C.20h | 153–350 | 73.6 (0.6) | 1.6×10^6 (11%) | 0.97 |
| | 352–585 | 70.9 (4.0) | 3.2×10^4 (51%) | 0.83 |
| HPL.20%.250C.20h | 188–350 | 94.8 (0.3) | 1.3×10^8 (12%) | 0.97 |
| | 442–546 | 236 (24) | 5.8×10^{16} (52%) | 0.93 |
| HPL.50%.250C.20h | 177–344 | 90.2 (0.8) | 6.3×10^7 (18%) | 0.97 |
| | 426–566 | 194 (5.8) | 6.9×10^{12} (106%) | 0.95 |
| PSS.350C.2h | 240–569 | 77.6 (1.7) | 5.0×10^4 (39%) | 0.90 |
| PSS.500C.2h | 284–560 | 107 | 5.5×10^6 | 0.91 |
| PPL.350C.2h | 235–585 | 60.1 (0.1) | 1.5×10^3 (5.9%) | 0.90 |
| PPL.500C.2h | 251–636 | 68 (1.4) | 5.1×10^3 (31%) | 0.93 |
| | 277–646 | 90.1 (1.4) | 1.5×10^5 (24%) | 0.94 |
| Coal1 | 277–646 | 90.1 (1.4) | 1.5×10^5 (24%) | 0.94 |
| Coal2 | 269–656 | 83.0 (1.7) | 4.7×10^4 (37%) | 0.93 |
| Coal3 | 269–663 | 84.9 (4.5) | 7.8×10^4 (61%) | 0.94 |
| Coal4 | 265–665 | 81.9 (3.6) | 4.3×10^4 (74%) | 0.93 |

^aMean of three replicates with standard deviation for E and coefficient of variation for A in parentheses. ^bcoefficient of variation (CV) = standard deviation/mean.

entirely with hydrochar, instead a blend of the two may be preferable.

Simulation of the Combustion Kinetics for Blends of Chars and Coal. In order to elucidate how the combustion characteristics will be affected by the blending of chars with coal for power generation, the combustion kinetics for two types of blends were simulated using the experimentally determined data, through superposition of two different feedstock TGA curves under the assumption that the individual feedstocks undergo independent combustion reactions without interaction.³⁹ The simulated TGA and DTG profiles of blends of one hydrochar (HSS.20%.200C.4h) and one pyrochar (PSS.500C.2h) with a fossil coal (Coal1) are shown in Figure 3. The resulting three combustion temperatures for the blends are listed in Table 4.

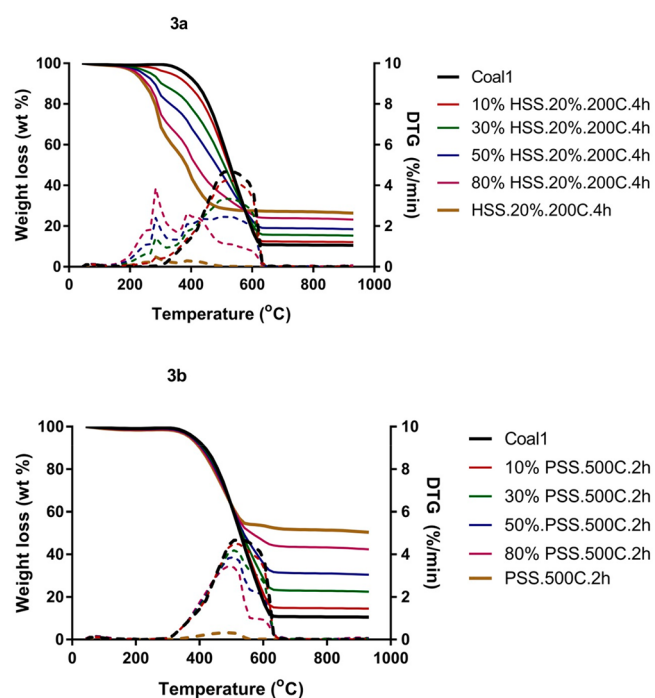


Figure 3. Simulated TGA and DTG profiles of blended coals; (a) hydrochar (HSS.20%.200C.4h) and (b) pyrochar (PSS.500C.2h) with a fossil coal (Coal1).

The DTG profiles for the coal-hydrochar blends are transformed from one broad peak of coal to two stages as the ratio of hydrochar is increased (Figure 3a). The early peak is due to decomposition of the higher VM of the hydrochar ahead of the coal, which lowers the ignition and peak temperatures compared to those of coal alone, enhancing combustion.⁴¹ Increasing the percentage of hydrochar above 30% causes a sharp drop in the peak temperature, whereas the burnout temperature first substantially decreases when an 80% blend is reached (Table 4). The DTG profiles of the pyrochar blends (Figure 3b), unlike hydrochar blends, do not see the development of two peaks as pyrochar is added. There is little change in the combustion characteristics until an 80% pyrochar blend is reached, when the burnout temperature decreases. The TGA profiles show that the ash content of the blends increases significantly due to the high ash content of the pyrochar. Although small synergistic combustion interactions between coal and torrefied biomass³¹ or sewage-sludge-derived hydrochars⁴² have been reported in the literature, the

Table 4. Simulated Combustion Characteristics of Blended Coals; Hydrochar or Pyrochar with a Fossil Coal (Coal1)

| samples | ignition temperature, T_{ig} (°C) | peak temperature, T_p (°C) | burnout temperature, T_b (°C) |
|-------------------------------------|-------------------------------------|------------------------------|---------------------------------|
| Hydrochar (HSS.20% \cdot 200C.4h) | 211 | 291 | 462 |
| 80% Hydrochar +20% Coal1 | 218 | 290 | 540 |
| 50% Hydrochar +50% Coal1 | 238 | 289 | 614 |
| 30% Hydrochar +70% Coal1 | 276 | 513 | 622 |
| 10% Hydrochar +90% Coal1 | 287 | 514 | 622 |
| Coal1 | 373 | 515 | 623 |
| Pyrochar (PSS.500C.2h) | 369 | 482 | 535 |
| 80% Pyrochar +20% Coal1 | 369 | 487 | 551 |
| 50% Pyrochar +50% Coal1 | 370 | 499 | 617 |
| 30% Pyrochar +70% Coal1 | 370 | 502 | 620 |
| 10% Pyrochar +90% Coal1 | 371 | 505 | 622 |
| Coal1 | 373 | 515 | 623 |

theoretical TG and DTG curves without any interactions are still useful to provide first-hand insights on cocombusting behaviors of swine-manure-derived hydrochars and pyrochars blended with coals. Further work is needed on actual blends to validate this assumption as a next step toward implementing co-combustion, but it is beyond the scope of this investigation.

In order to decide which of the two thermochemical conversion processes studied here will produce a better solid fuel from the two animal manures, further experiments that consider the wide variation in feedstock characteristics should be made with focus on influencing the ash content and composition, as well as carbonization conditions. One advantage for pyrochar is that blends of pyrochar can be used in existing coal-burning facilities since there is not much change in the ignition temperature. However, the results in Table 1 show that the energy recovered via hydrothermal carbonization was higher than that for pyrolysis (53–76% vs 41–60%). This higher energy yield for hydrochar combined with the advantage of its high VM contents which promotes ignition (i.e., considerably lower ignition temperature than that of coal) may make HTC more competitive for installations designed for renewable fuels. The changes in the combustion temperatures should not present a hindrance for the use of hydrochar blends in the power generation industry, where biomasses with similar values are currently being used^{43,44} (e.g., wood chips or straw). In order to exploit the changes in combustion characteristics due to hydrochar, the operating conditions of the power plant could be adjusted for improved combustion. Some of the main adjustments could be the residence time of the fuel in the combustion chamber for the case of “moving grate” boilers, or controlling the air stream for an effective excess air ratio.

Moreover, the use of animal manure hydrochars as a substitute for traditional noncarbonized biomasses can expand the sources of renewable fuels and reduce negative impacts from localized excess manure production in CAFOs. The thermochemical conversion stabilizes and reduces the volume of the solids to be transported. Although further research on operational challenges in combustion with high ash-containing chars and potential environmental impacts (offgas, ash utilization) is needed, such treatment can reduce transportation costs, and the resulting hydrochars can increase combustion reactivity in fossil coal blends.

CONCLUSIONS

This investigation highlights the potential of the two thermochemical processes (hydrothermal carbonization and

pyrolysis) to convert surplus manure waste streams into renewable fuels. Co-combustion of manure-derived chars in existing coal-fired power plants can increase the sustainability of energy production as well as manure management systems. The thermogravimetric analysis showed that the hydrochars underwent two combustion stages, active and char combustion, while only one stage was seen for the pyrochars and four fossil coals. The activation energies calculated for the swine-manure-derived hydrochars were generally smaller than those of the four coals. Poultry-litter-derived hydrochars required higher activation energies than those of the coals. The substantial differences in characteristic combustion temperatures, ash contents, and the kinetics between hydrochar and actual coal samples suggest that the fossil coals used by existing coal power plants should not be replaced entirely with hydrochar, but preferably as a blend. On the basis of the results from the simulated hydrochar/coal blends, we conclude that hydrochar blends (10% or less) with coal will not significantly change combustion characteristics nor ash amounts for existing power plants. More research is needed to elucidate the detailed reaction mechanisms and to determine optimal blend ratios of different hydrochars to be used for power generation. In contrast, the combustion characteristics of animal-manure pyrochars were not substantially different from that of coals. However, blending high percentages of animal-manure pyrochars would substantially increase ash contents, complicating downstream ash management practices. As there is a high variation in the raw material properties of manure coming from different livestock operations, further experiments that consider the wide variation in feedstock characteristics are necessary in order to decide which of the two thermochemical conversion processes studied here will produce a better solid fuel.

AUTHOR INFORMATION

Corresponding Author

*E-mail: kyoung.ro@ars.usda.gov.

ORCID

Kyoung S. Ro: [0000-0002-2622-8279](https://orcid.org/0000-0002-2622-8279)

Notes

The authors declare no competing financial interest.

ACKNOWLEDGMENTS

The authors would like to acknowledge the technical support provided by Mr. Melvin Johnson, Mr. Jerry H. Martin of the USDA-ARS Coastal Plains Soil, Water, Plant Research Center,

Florence, SC. This research was supported by the USDA-ARS National Programs 212 and 214. Mention of trade names or commercial products is solely for the purpose of providing specific information and does not imply recommendation or endorsement by the U.S. Department of Agriculture.

REFERENCES

- (1) Bolan, N. S.; Szogi, A. A.; Chuasavathi, T.; Seshadri, B.; Rothrock, M. J., Jr.; Panneerselvam, P. Uses and management of poultry litter. *World's Poult. Sci. J.* **2010**, *66* (4), 673–698.
- (2) Weinfurter, K. *Matrix parameters and storage conditions of manure*; Report No. UBA-FB 001436/E; Federal Environment Agency: Dessau, Germany, 2011.
- (3) Park, M.-H.; Kumar, S.; Ra, C. Solid waste from swine wastewater as a fuel source for heat production. *Asian-Australas. J. Anim. Sci.* **2012**, *25* (11), 1627–1633.
- (4) Chastain, J. P.; Coloma-del Valle, A.; Moore, K. P. Using broiler litter as an energy source: Energy content and ash composition. *Appl. Eng. Agric.* **2012**, *28* (4), 513–522.
- (5) Sharara, M. A.; Sadaka, S. S.; Costello, T. A.; VanDevender, K.; Carrier, J.; Popp, M.; Thoma, G.; Djiroleu, A. Combustion kinetics of swine manure and algal solids. *J. Therm. Anal. Calorim.* **2016**, *123* (1), 687–696.
- (6) Bemhart, M. E.; Fasina, O. Physical properties and pyrolysis behavior of fractionated poultry litter. *Trans. ASABE* **2009**, *52* (2), 531–538.
- (7) Cantrell, K.; Ro, K.; Mahajan, D.; Anjom, M.; Hunt, P. G. Role of thermochemical conversion in livestock waste-to-energy treatments: Obstacles and opportunities. *Ind. Eng. Chem. Res.* **2007**, *46* (26), 8918–8927.
- (8) Cantrell, K. B.; Ducey, T. F.; Ro, K. S.; Hunt, P. G. Livestock waste-to-bioenergy generation opportunities. *Bioresour. Technol.* **2008**, *99* (17), 7941–7953.
- (9) Kirubakaran, V.; Sivaramkrishnan, V.; Premalatha, M.; Subramanian, P. Kinetics of auto-gasification of poultry litter. *Int. J. Green Energy* **2007**, *4*, 519–534.
- (10) Lima, I. M.; Boateng, A. A.; Klasson, K. T. Pyrolysis of broiler manure: char and product gas characterization. *Ind. Eng. Chem. Res.* **2009**, *48*, 1292–1297.
- (11) Priyadarsan, S.; Annamalai, K.; Sweeten, J. M.; Mukhtar, S.; Holtzapple, M. T. Fixed-bed gasification of feedlot manure and poultry litter biomass. *Trans. ASABE* **2004**, *47* (5), 1689.
- (12) Ro, K. S. Kinetics and energetics of producing animal manure-based biochar. *BioEnergy Res.* **2016**, *9*, 447–453.
- (13) Ro, K. S.; Cantrell, K. B.; Elliott, D.; Hunt, P. G. Catalytic Wet Gasification of Municipal and Animal Wastes. *Ind. Eng. Chem. Res.* **2007**, *46*, 8839–8845.
- (14) Ro, K. S.; Cantrell, K. B.; Hunt, P. G. High-temperature pyrolysis of blended animal manures for producing renewable energy and value-added biochar. *Ind. Eng. Chem. Res.* **2010**, *49*, 10125–10131.
- (15) Ro, K. S.; Cantrell, K. B.; Hunt, P. G.; Ducey, T. F.; Vanotti, M. B.; Szogi, A. A. Thermochemical conversion of livestock wastes: Carbonization of swine solids. *Bioresour. Technol.* **2009**, *100*, 5466–5471.
- (16) Ro, K. S.; Hunt, P. G.; Jackson, M. A.; Compton, D. L.; Yates, S. R.; Cantrell, K.; Chang, S. C. Co-pyrolysis of swine manure with agricultural plastic waste: laboratory-scale study. *Waste Manage.* **2014**, *34*, 1520–1528.
- (17) Sheth, A. C.; Turner, A. D. Kinetics and economics of catalytic steam gasification of broiler litter. *Trans. ASABE* **2002**, *45* (4), 1111–1121.
- (18) Young, L.; Pian, C. C. P. High-temperature, air-blown gasification of dairy-farm wastes for energy production. *Energy* **2003**, *28* (7), 655–672.
- (19) Stephenson, A. H.; McCaskey, T. A.; Ruffin, B. G. A survey of broiler litter composition and potential value as a nutrient resource. *Biol. Wastes* **1990**, *34* (1), 1–9.
- (20) Zhu, N. Composting of high moisture content swine manure with corn cob in a pilot-scale aerated static bin system. *Bioresour. Technol.* **2006**, *97*, 1870–1875.
- (21) Teixeira, P.; Lopes, H.; Gulyurtlu, I.; Lapa, N.; Abelha, P. Evaluation of slagging and fouling tendency during biomass co-firing with coal in a fluidized bed. *Biomass Bioenergy* **2012**, *39*, 192–203.
- (22) Niu, Y.; Zhu, Y.; Tan, H.; Hui, S.; Jing, Z.; Xu, W. Investigations on biomass slagging in utility boiler: Criterion numbers and slagging growth mechanisms. *Fuel Process. Technol.* **2014**, *128*, 499–508.
- (23) Brunner, T.; Wohlmuther, M.; Kanzian, W.; Obernberger, I.; Pichler, W. Additive guideline - How to utilize inorganic additives as a measure to improve combustion related properties of agricultural biomass fuels. *23rd European Biomass Conference and Exhibition*, Vienna, Austria, June 1–4, 2015.
- (24) Libra, J. A.; Ro, K. S.; Kammann, C.; Funke, A.; Berge, N. D.; Neubauer, Y.; Titirici, M. M.; Fuhner, C.; Bens, O.; Kern, J.; Emmerich, K.-H. Hydrothermal carbonization of biomass residuals: a comparative review of the chemistry, processes and applications of wet and dry pyrolysis. *Biofuels* **2011**, *2* (1), 71–106.
- (25) Berge, N. D.; Kammann, C.; Ro, K. S.; Libra, J. A. *Environmental Applications of Hydrothermal Carbonization Technology: Biochar Production, Carbon Sequestration, and Waste Conversion*; John Wiley & Sons, Inc.: West Sussex, U.K., 2013.
- (26) Li, L.; Flora, J. R. V.; Caicedo, J. M.; Berge, N. D. Investigating the role of feedstock properties and process conditions on products formed during the hydrothermal carbonization of organics using regression techniques. *Bioresour. Technol.* **2015**, *187*, 263–274.
- (27) Cao, X.; Ro, K. S.; Chappell, M.; Li, Y.; Mao, J. Chemical structures of swine-manure chars produced under different carbonization conditions investigated by advanced solid-state ^{13}C nuclear magnetic resonance (NMR) spectroscopy. *Energy Fuels* **2011**, *25*, 388–397.
- (28) Mau, V.; Gross, A. Energy conversion and gas emissions from production and combustion of poultry-litter-derived hydrochar and biochar. *Appl. Energy* **2018**, *213*, 510–519.
- (29) Priyanto, D. E.; Matsunaga, Y.; Ueno, S.; Kasai, H.; Tanoue, T.; Mae, K.; Fukushima, H. Co-firing high ratio of woody biomass with coal in a 150-MW class pulverized coal boiler: Properties of the initial deposits and their effect on tube corrosion. *Fuel* **2017**, *208*, 714–721.
- (30) Li, J.; Brzdekiewicz, A.; Yang, W.; Blasiak, W. Co-firing based on biomass torrefaction in a pulverized coal boiler with aim of 100% fuel switching. *Appl. Energy* **2012**, *99*, 344–354.
- (31) Toptas, A.; Yildirim, Y.; Duman, G.; Yanik, J. Combustion behavior of different kinds of torrefied biomass and their blends with lignite. *Bioresour. Technol.* **2015**, *177*, 328–336.
- (32) Ro, K. S.; Flora, J. R. V.; Bae, S.; Libra, J. A.; Berge, N. D.; Álvarez-Murillo, A.; Li, L. Properties of animal-manure-based hydrochars and predictions using published models. *ACS Sustainable Chem. Eng.* **2017**, *5*, 7317–7324.
- (33) Cantrell, K. B.; Martin, J. H. Stochastic state-space temperature regulation of biochar production. Part II: Application to manure processing via pyrolysis. *J. Sci. Food Agric.* **2012**, *92* (3), 490–495.
- (34) Dean, S. W.; Cantrell, K. B.; Martin, J. H.; Ro, K. S. Application of thermogravimetric analysis for the proximate analysis of livestock wastes. *J. ASTM Int.* **2010**, *7*, 102583.
- (35) ASTM. *Petroleum Products, Lubricants, and Fossil Fuels: Gaseous Fuels, Coal, And Coke*. ASTM International: West Conshohocken, PA, 2006.
- (36) Meng, F.; Yu, J.; Tahmasebi, A.; Han, Y. Pyrolysis and combustion behavior of coal gangue in O_2/CO_2 and O_2/N_2 mixtures using thermogravimetric analysis and a drop tube furnace. *Energy Fuels* **2013**, *27*, 2923–2932.
- (37) Park, S.-W.; Jang, C.-H. Effects of pyrolysis temperature on changes in fuel characteristics of biomass char. *Energy* **2012**, *39*, 187–195.
- (38) Cantrell, K. B.; Hunt, P. G.; Ro, K. S.; Stone, K. C.; Vanotti, M. B.; Burns, J. C. Thermogravimetric characterization of irrigated

bermudagrass as a combustion feedstock. *Trans. ASABE* **2010**, *53* (2), 413–420.

(39) Garcia-Nunez, J. A.; Garcia-Perez, M.; Das, K. C. Determination of kinetic parameters of thermal degradation of palm oil mill by-products using thermogravimetric analysis and differential scanning calorimetry. *Trans. ASABE* **2008**, *51* (2), 547–557.

(40) Makela, M.; Yoshikawa, K. Ash behavior during hydrothermal treatment for solid fuel applications. Part 2: Effects of treatment conditions on industrial waste biomass. *Energy Convers. Manage.* **2016**, *121*, 409–414.

(41) Wang, Z.; Hong, C.; Xing, Y.; Li, Y.; Feng, L.; Jia, M. Combustion behaviors and kinetics of sewage sludge blended with pulverized coal: With and without catalysts. *Waste Manage.* **2018**, *74*, 288–296.

(42) He, C.; Wang, K.; Yang, Y.; Wang, J.-Y. Utilization of sewage-sludge-derived hydrochars toward efficient cocombustion with different-rank coals: effects of subcritical water conversion and blending scenarios. *Energy Fuels* **2014**, *28*, 6140–6150.

(43) Al-Mansour, F.; Zuwala, J. An evaluation of biomass co-firing in Europe. *Biomass Bioenergy* **2010**, *34* (5), 620–629.

(44) Agbor, E.; Zhang, X.; Kumar, A. A review of biomass co-firing in North America. *Renewable Sustainable Energy Rev.* **2014**, *40*, 930–943.